Cell Reports

Report

Feedback Inhibition of the Rag GTPase GAP Complex Lst4-Lst7 Safeguards TORC1 from Hyperactivation by Amino Acid Signals

Graphical Abstract

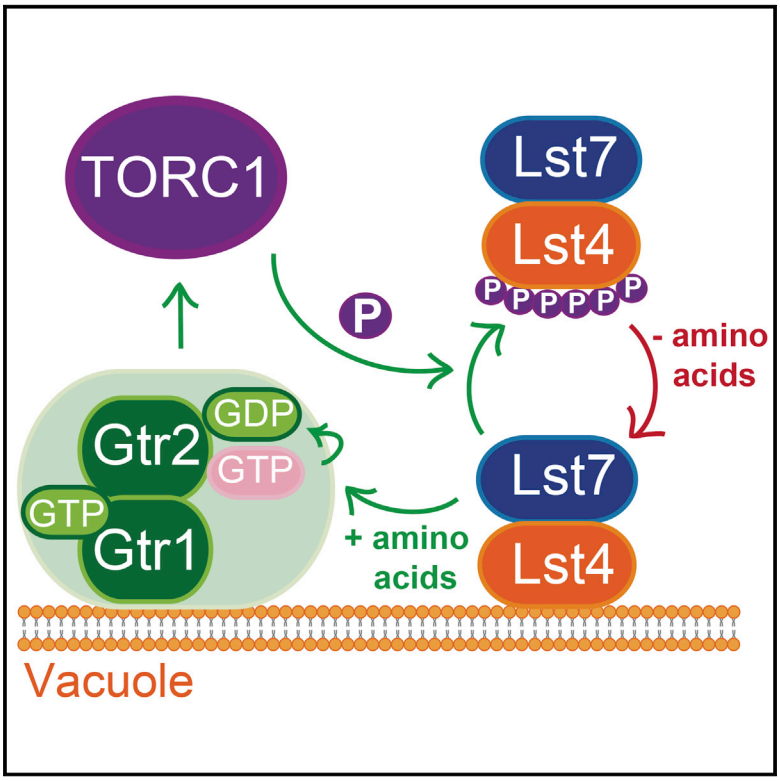

Authors

Marie-Pierre Péli-Gulli, Serena Raucci, Zehan Hu, Jörn Dengjel, Claudio De Virgilio

Correspondence

claudio.devirgilio@unifr.ch

In Brief

Amino acids activate Rag GTPase-TORC1 signaling in part through the conserved Lst4-Lst7 Rag GTPase GAP complex. Here, Péli-Gulli et al. show that the Lst4-Lst7 module is a direct TORC1 target and key node of a feedback mechanism that adjusts TORC1 activity to amino acid availability.

Highlights

- Amino acids activate the Lst4-Lst7-Rag GTPase-TORC1 branch at the vacuolar membrane
- The Lst4 intra-DENN loop is required and sufficient for its membrane tethering
- TORC1 phosphorylates this loop to disperse the Lst4-Lst7 complex from the vacuole
- This feedback inhibition prevents TORC1 hyperactivation and is relevant for growth

Péli-Gulli et al., 2017, Cell Reports *20*, 281–288
July 11, 2017 © 2017 The Author(s).
http://dx.doi.org/10.1016/j.celrep.2017.06.058

CellPress

Cell Reports
Report

OPEN ACCESS
CellPress

Feedback Inhibition of the Rag GTPase GAP Complex Lst4-Lst7 Safeguards TORC1 from Hyperactivation by Amino Acid Signals

Marie-Pierre Péli-Gulli,[1,2] Serena Raucci,[1,2] Zehan Hu,[1] Jörn Dengjel,[1] and Claudio De Virgilio[1,3,*]
[1]Department of Biology, University of Fribourg, CH-1700 Fribourg, Switzerland
[2]These authors contributed equally
[3]Lead Contact
*Correspondence: claudio.devirgilio@unifr.ch
http://dx.doi.org/10.1016/j.celrep.2017.06.058

SUMMARY

Amino acids stimulate the eukaryotic target of rapamycin complex 1 (TORC1), and hence growth, through the Rag GTPases and their regulators. Among these, the yeast Lst4-Lst7 Rag GTPase GAP complex clusters, as we previously reported, at the vacuolar membrane upon amino acid starvation. In response to amino acid refeeding, it activates the Rag GTPase-TORC1 branch and is then dispersed from the vacuolar surface. Here, we show that the latter effect is driven by TORC1 itself, which directly phosphorylates several residues within the intra-DENN loop of Lst4 that, only in its non-phosphorylated state, tethers the Lst4-Lst7 complex to the vacuolar membrane. An Lst4 variant disrupting this feedback inhibition mechanism causes TORC1 hyperactivation and proliferation defects in cells grown on poor nitrogen sources. Thus, we identify Lst4 as a TORC1 target and key node of a homeostatic mechanism that adjusts TORC1 activity to the availability of amino acids.

INTRODUCTION

The eukaryotic target of rapamycin complex 1 (TORC1) is a homeostatic controller of cell growth that adjusts anabolic and catabolic processes to diverse environmental signals, and aberrant mammalian TORC1 (mTORC1) signaling contributes to the progression of human diseases such as cancer and diabetes (Albert and Hall, 2015; Eltschinger and Loewith, 2016; Saxton and Sabatini, 2017). Amino acids are important signals that control TORC1 function via the conserved, heterodimeric Rag family of GTPases (i.e., yeast Gtr1 combined with Gtr2 or mammalian RagA or RagB combined with RagC or RagD) (Binda et al., 2009; Jewell et al., 2013; Kim et al., 2008; Sancak et al., 2008; Sancak and Sabatini, 2009). Rag GTPase heterodimers stimulate TORC1 when they contain GTP-loaded Gtr1/RagA/B and GDP-loaded Gtr2/RagC/D, a configuration that is promoted in part by the GTPase activating protein (GAP) complex Lst4-Lst7 that acts on Gtr2 or the orthologous FNIP1/2-Folliculin (FLCN) complex that acts on RagC/D (Péli-Gulli et al., 2015; Petit et al., 2013; Tsun et al., 2013). How amino acids activate TORC1 through these GAP complexes is currently not known (Hatakeyama and De Virgilio, 2016).

Whereas much attention has been focused on the mechanisms by which amino acids activate (or by which their absence inactivates) the Rag GTPase-TORC1 branch (Powis and De Virgilio, 2016; Saxton and Sabatini, 2017), recent data indicate the presence of additional regulatory layers such as feedback control loops that allow cells to rapidly and dynamically adjust TORC1 activity to changing levels of extracellular amino acids. In mammalian cells, for instance, amino acid-mediated stimulation of the RagA-mTORC1 interaction (and consequently lysosomal membrane recruitment and activation of mTORC1 by Rheb; Saxton and Sabatini, 2017) is likely attenuated by a negative feedback through Skp2-dependent RagA ubiquitination, which recruits GATOR1 to prevent mTORC1 hyperactivation (Jin et al., 2015). Because amino acid stimulation results in transient, Gtr1-dependent hyperactivation of vacuolar membrane-resident TORC1 in cells pregrown on nitrogen-poor media (Stracka et al., 2014), an analogous mechanism may also exist in yeast. In addition, alternative feedback circuits may also act through the Lst4-Lst7 GAP complex, which exhibits only a short-lived preference for Gtr2-binding following re-stimulation of cells with glutamine (Péli-Gulli et al., 2015).

Here, we report on our finding that Lst4 is a bona fide target of TORC1 in yeast and that the TORC1-mediated phosphorylation events on Lst4 serve to disperse the Lst4-Lst7 GAP complex from the vacuolar membrane to attenuate its stimulatory effects on Gtr2 and consequently TORC1 itself in glutamine-fed cells. Replacement of Lst4 residues phosphorylated by TORC1 with alanines results in constitutive vacuolar-membrane recruitment of Lst4-Lst7, which causes TORC1 hyperactivation in glutamine-stimulated cells and growth defects when cells are cultivated on nitrogen-poor media. Conversely, an Lst4 variant mimicking its TORC1-phosphorylated state, despite being fully capable of forming a functional GAP complex with Lst7, is unable to deliver the complex to the vacuolar membrane and fails to mediate amino acid-dependent TORC1 activation. Thus, our study identifies a physiologically relevant negative feedback mechanism that restricts TORC1 signaling upon sustained glutamine stimulation.

This is an open access article under the CC BY-NC-ND license (http://creativecommons.org/licenses/by-nc-nd/4.0/).

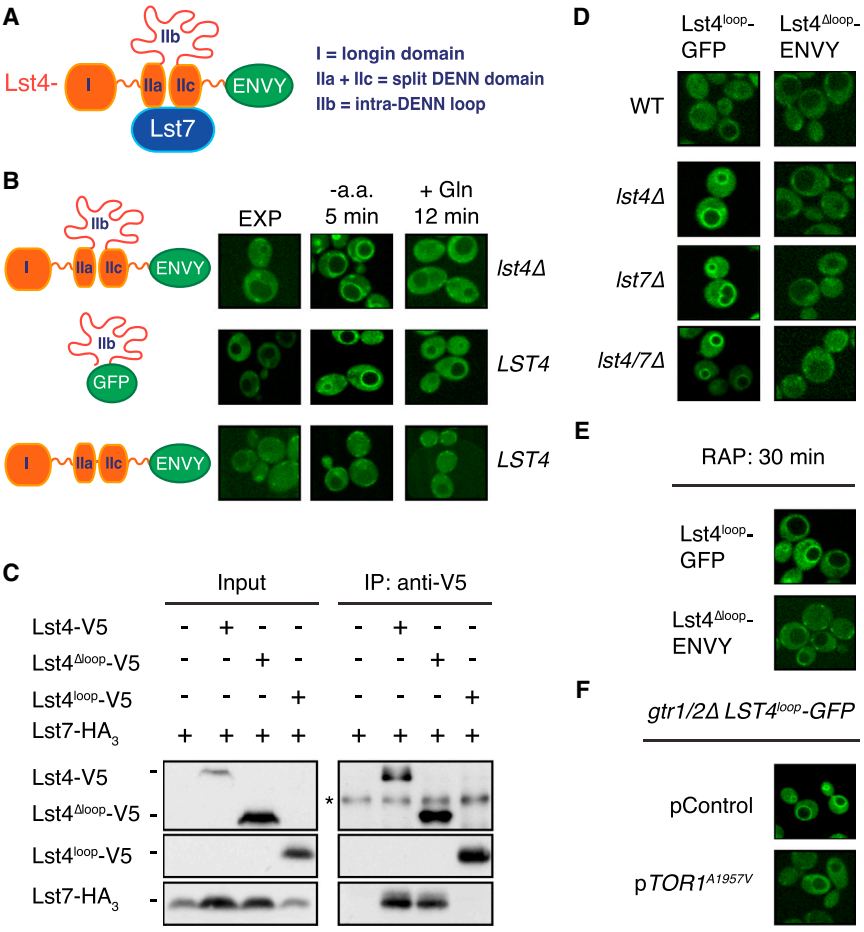

Figure 1. The Lst4 Intra-DENN Loop Is Necessary and Sufficient for Regulated Vacuolar Membrane Tethering

(A) Domain architecture of Lst4 (according to Pacitto et al., 2015). I, longin domain; IIa and IIc, Lst7-binding, split DENN domain; IIb, unstructured intra-DENN loop. Lst4 is represented fused to ENVY, a GFP moiety variant.

(B) Lst4^{loop}-GFP, but not Lst4$^{\Delta loop}$-ENVY, exhibits dynamic redistribution upon amino acid starvation and glutamine refeeding. Indicated strains genomically expressed Lst4-ENVY and Lst4$^{\Delta loop}$-ENVY from the *LST4* promoter or Lst4^{loop}-GFP from the *CYC1* promoter. Cells were cultured exponentially in SC medium (EXP), starved of amino acids for 5 min (-a.a.; 5 min), and restimulated with 3 mM glutamine for 12 min (+ Gln; 12 min).

(C) The Lst4^{loop} is dispensable for the interaction between Lst4 and Lst7. *lst7Δ* cells expressing plasmid-encoded Lst7-HA$_3$ and co-expressing (+) or not (-) the indicated plasmid-encoded Lst4-V5 variants were grown exponentially in SC. Lysates (input) and anti-V5 immunoprecipitates (IP: anti-V5) were analyzed by immunoblotting with anti-HA and anti-V5 antibodies. The asterisk denotes a cross-reacting band.

(D) Lst4^{loop}-GFP, but not Lst4$^{\Delta loop}$-ENVY, accumulates at the vacuolar surface of *lst4Δ*, *lst7Δ*, or *lst4/7Δ* cells. Indicated strains expressing either Lst4^{loop}-GFP or Lst4$^{\Delta loop}$-ENVY as in (B) were grown exponentially in SC. WT, wild-type.

(E) Lst4$^{\Delta loop}$-ENVY is not recruited to the vacuolar membrane following rapamycin treatment. Lst4^{loop}-GFP- or Lst4$^{\Delta loop}$-ENVY-expressing wild-type cells were grown exponentially in SC and then treated with rapamycin for 30 min.

(F) Expression of hyperactive *TOR1*^{A1957V} disperses the Lst4^{loop}-GFP from the vacuolar membrane in *gtr1Δ gtr2Δ* cells. Cells (indicated genotype) expressing or not (pControl) plasmid-encoded *TOR1*^{A1957V} (*pTOR1*^{A1957V}) were grown exponentially in SC.

RESULTS AND DISCUSSION

The Intra-DENN Loop Is Necessary and Sufficient for Regulated Vacuolar Membrane Targeting of Lst4

We previously observed that the Lst4-Lst7 heterodimer, like mammalian FNIP1/2-FLCN, clusters at and is released from the vacuolar membrane upon amino acid starvation and refeeding, respectively (Péli-Gulli et al., 2015; Petit et al., 2013; Tsun et al., 2013). To address the mechanistic basis of this dynamic regulation of the Lst4-Lst7 complex localization, we initially studied the potential role in this process of the unstructured loop within the DENN (differentially expressed in normal and neoplastic cells) domain of Lst4 (encompassing amino acids 400–600 of Lst4 and referred to as Lst4^{loop} hereafter), which splits the Lst7-interacting DENN domain of Lst4 into two halves (Pacitto et al., 2015) (Figure 1A). Like Lst4-ENVY (or Lst4-GFP; see Péli-Gulli et al., 2015), the Lst4^{loop}-GFP construct localized mainly within the cytoplasm of exponentially growing cells, was rapidly recruited to the vacuolar membrane upon starvation of cells for amino acids, and dispersed back to the cytoplasm upon refeeding of cells with glutamine, which is specifically potent for that matter (Figure 1B). An Lst4 ENVY-fusion protein lacking the Lst4^{loop} region (Lst4$^{\Delta loop}$-ENVY), in contrast, remained constitutively cytoplasmic in similar experiments, indicating that the Lst4^{loop} is both necessary and sufficient to mediate the amino acid starvation-induced vacuolar membrane recruitment of Lst4. Of note, control co-immunoprecipitation experiments revealed that the Lst4^{loop} was not required for Lst4 to associate with Lst7 (Figure 1C), as also described earlier (Pacitto et al., 2015). Combined with the fact that Lst7 depends on Lst4 for its vacuolar membrane recruitment (Péli-Gulli et al., 2015), the Lst4^{loop} appears therefore to primarily function in dynamically regulating the localization, but not the Gtr2 GAP function per se (see also below), of the entire Lst4-Lst7 complex.

Previously published data suggested that TORC1 antagonizes the vacuolar enrichment of the Lst4-Lst7 complex by a mechanism that remained unexplored (Péli-Gulli et al., 2015). We suspected therefore that TORC1 might exert its effect on the localization of Lst4-Lst7 by regulating (directly or indirectly) the function of the Lst4^{loop}. In support of this idea, we found interventions that reduce TORC1 activity, such as individual or combined loss of Lst4 and Lst7, combined loss of Gtr1 and Gtr2, and rapamycin treatment to trigger the enrichment of the Lst4^{loop}-GFP, but not that of the Lst4$^{\Delta loop}$-GFP, at the vacuolar membrane

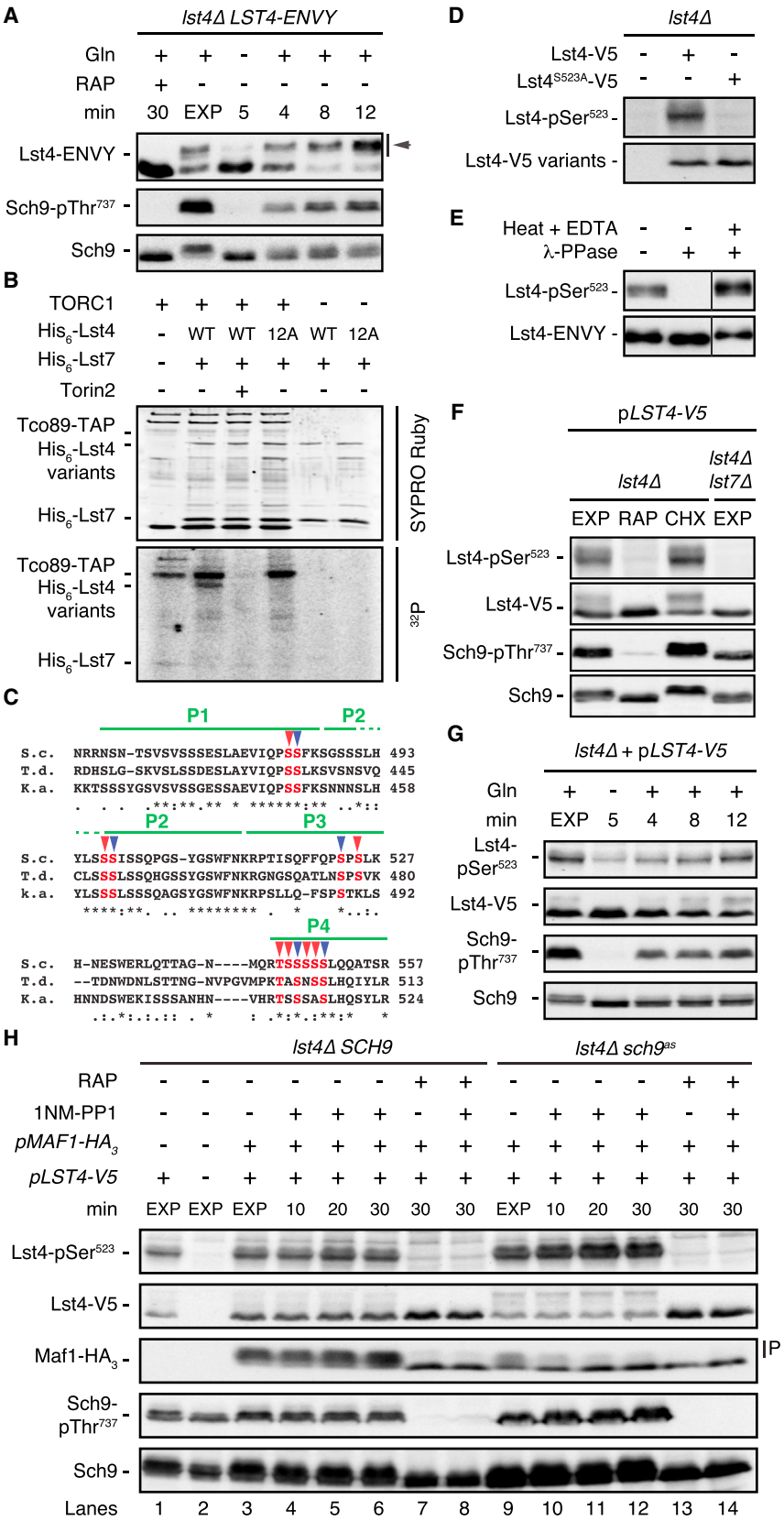

Figure 2. Lst4 Is Phosphorylated In Vivo and In Vitro by TORC1

(A) Lst4-ENVY phosphorylation mirrors TORC1 activation. Lst4-ENVY-expressing *lst4Δ* cells were grown in SC. They were either left untreated (EXP), treated with rapamycin for 30 min (RAP; 30 min), or starved of amino acids for 5 min (-; 5 min) and re-stimulated with 3 mM glutamine for the indicated times (+ Gln; 4–12 min). Phosphorylation of Lst4-ENVY was analyzed on a phostag gel followed by immunoblotting with anti-GFP antibodies. For comparison, phosphorylation of the TORC1 target residue Thr^{737} within Sch9 (Urban et al., 2007) was monitored by immunoblot analysis using anti-Sch9-$pThr^{737}$ and anti-Sch9 antibodies. The arrow points to hyperphosphorylated isoforms of Lst4-ENVY.

(B) TORC1 phosphorylates Lst4 in vitro. Purified recombinant His_6-Lst4/His_6-Lst7 (WT) and His_6-$Lst4^{12A}$/His_6-Lst7 (12A) were subjected to in vitro phosphorylation by TORC1 (purified from yeast) in the absence (-) or presence (+) of the TOR inhibitor Torin2. Representative SYPRO Ruby staining and autoradiography (^{32}P) blots are shown.

(C) TORC1 phosphorylates multiple residues within the intra-DENN loop of Lst4. A multiple sequence alignment of a part of the intra-DENN loop of Lst4 from *S. cerevisiae* (S.c.), *Torulaspora delbrueckii* (T.d.), and *Kazachstania africana* (K.a.) is shown. Mass spectrometric analysis of Lst4, which has been phosphorylated in vitro by purified TORC1, identified four different phosphopeptides (P1–4) with 12 potentially phosphorylated Ser (S)/Thr (T) residues (arrowheads; see Table S3). The 12 Ser/Thr residues that were mutated to Ala in the $Lst4^{12A}$ allele are marked with red or blue arrowheads, while the 5 Ser residues mutated to Asp in the $Lst4^{5D}$ allele are indicated only with blue arrowheads.

(D) Specificity of the anti-Lst4-$pSer^{523}$ antibodies. *lst4Δ* expressing, or not (-), plasmid-encoded Lst4-V5 or $Lst4^{S523A}$-V5 (+) were grown exponentially in SC, and the respective extracts were assayed by immunoblot analysis using anti-Lst4-$pSer^{523}$ and anti-V5 antibodies.

(E) Lst4-ENVY was immunoprecipitated from exponentially growing *lst4Δ* cells and then treated (+), or not (-), with λ-phosphatase (λ-PPase), which was (+), or was not (-), inactivated by heat (65°; 30 min) in the presence of EDTA prior to use. Immunoprecipitates were analyzed by immunoblotting using anti-Lst4-$pSer^{523}$ and anti-GFP antibodies.

(F) Lst4 phosphorylation on Ser^{523} (Lst4-$pSer^{523}$) mirrors TORC1 activation and requires the presence of Lst7. *lst4Δ* or *lst4Δ lst7Δ* strains expressing plasmid-encoded Lst4-V5 were grown exponentially in SC (EXP) and then treated with rapamycin (RAP) or cycloheximide (CHX) for 30 min. Lst4-$pSer^{523}$ and Sch9-$pThr^{737}$ were analyzed as in (D) and (A), respectively.

(G) Amino acid starvation and glutamine refeeding decrease and induce, respectively, the phosphorylation of Ser^{523} in Lst4. Cells (*lst4Δ*) expressing plasmid-encoded Lst4-V5 were treated as in (A). Lst4-$pSer^{523}$ and Sch9-$pThr^{737}$ were analyzed as in (F). See also Figure S1.

(H) Phosphorylation of Ser^{523} in Lst4 does not require Sch9. *lst4Δ SCH9* cells and *lst4Δ sch9Δ* cells that expressed the plasmid-encoded,

(legend continued on next page)

(Figures 1D and 1E). The expression of the hyperactive *TOR1*^{A1957V} allele (Reinke et al., 2006), in contrast, dispersed the Lst4^{loop}-GFP from the vacuolar membrane in *gtr1/2Δ* cells (Figure 1F). The vacuolar membrane recruitment of the Lst4^{loop}-GFP occurs therefore independently of the presence of Lst4-Lst7 or Gtr1-Gtr2 and is negatively regulated by TORC1.

The Lst4^{loop} Harbors Multiple TORC1 Phosphorylation Sites

Phostag gel electrophoresis separated Lst4-ENVY from extracts of exponentially growing wild-type cells into two roughly equal populations of fast and slowly migrating isoforms (Figure 2A). The levels of the latter, which we assumed corresponded to hyperphosphorylated variants of Lst4-ENVY, closely correlated with TORC1 activity, being barely detectable in rapamycin-treated and amino acid-starved cells but rapidly induced upon readdition of glutamine to starved cells (Figure 2A). To test whether Lst4 is a direct substrate of TORC1, a model we deemed feasible on the basis of both our present results and the reported spatial proximity of Lst4 and TORC1 at the vacuolar membrane (Binda et al., 2009; Péli-Gulli et al., 2015; Sturgill et al., 2008), we asked whether Lst4 could be a substrate of TORC1 in vitro. Indeed, TORC1 (purified from yeast) phosphorylated recombinant Lst4 (co-purified with Lst7) in the absence but not in the presence of the ATP-competitive TOR inhibitor Torin2 (Liu et al., 2013) (Figure 2B). Mass spectrometry (MS) analysis of the respective phosphorylated Lst4 protein allowed us to identify 4 non-overlapping phosphopeptides covering neighboring amino acid stretches within the intra-DENN loop of Lst4 with 12 potential phospho-Ser/Thr residues (see Table S3), many of which appeared to be conserved in closely related yeast species (Figure 2C). Because TORC1 was unable to phosphorylate in vitro an Lst4^{12A} variant in which these 12 Ser/Thr residues were substituted with Ala (Figure 2B), these 12 residues encompass the majority of residues in Lst4 that are modified by TORC1. To determine whether TORC1 also phosphorylates Lst4 in vivo, we used antibodies that recognized 1 of these 12 residues in Lst4 (i.e., Ser^{523}) specifically in its phosphorylated state (Figures 2D and 2E). Accordingly, we found that rapamycin-mediated TORC1 inhibition abolished whereas cycloheximide-mediated TORC1 activation (Binda et al., 2009) induced the phosphorylation of Ser^{523} within Lst4 (Lst4-pSer^{523}), as observed for the bona fide TORC1 target residue Thr^{737} in Sch9 (Sch9-pThr^{737}) (Urban et al., 2007) (Figure 2F). In addition, physiological interventions such as starvation for amino acids and glutamine refeeding also decreased and induced, respectively, both Lst4-pSer^{523} and Sch9-pThr^{737} levels with similar dynamics (Figure 2G). Moreover, glutamine refeeding failed to stimulate Lst4-Ser^{523} phosphorylation in the presence of rapamycin and did not significantly alter the levels of Lst4 (Figures S1A and S1B).

Although our in vitro and in vivo experiments pinpointed Lst4 as a direct TORC1 target, we considered it still formally possible that TORC1 controls Lst4 phosphorylation indirectly via Sch9. To address this point, we performed additional control experiments using a strain that expressed an ATP analog (1NM-PP1) sensitive Sch9^{as} variant (Huber et al., 2009). Because of the hypomorphic nature of this mutant allele (Huber et al., 2009), exponentially growing cells of the respective strain showed decreased basal phosphorylation levels of the Sch9 target Maf1 (i.e., lower levels of the slowly migrating, hyperphosphorylated Maf1 isoforms; compare lanes 3 and 9 in Figure 2H) that could be further reduced by 1NM-PP1 treatment (Figure 2H, lanes 10–12). Remarkably, however, *sch9*^{as} cells exhibited strongly increased basal levels of both Lst4-pSer^{523} and Sch9-pThr^{737} that were even further boosted by 1NM-PP1 treatment (Figure 2H, lanes 10–12). These results not only imply that Sch9 downregulation triggers TORC1 activation via a hitherto undescribed feedback mechanism but also exclude the involvement of Sch9 in direct phosphorylation of Lst4 (see also Figure S2). All of our data combined therefore confirm Lst4 as a bona fide target of TORC1.

Lst4 and Lst7 depend on each other for their assembly on the vacuolar membrane (Péli-Gulli et al., 2015). On the basis of our present observations and recent structural studies of Lst4 (Pacitto et al., 2015), this is likely explained by the fact that Lst7 binds to and consequently reunites the separated parts of the Lst4 split DENN domain, thereby also ensuring the proper folding of the intra-DENN loop of Lst4, which drives the joint recruitment of Lst4 and Lst7 to the vacuolar membrane (Figure 1A). Our results therefore predicted that loss of Lst7 should deprive the vacuolar membrane-resident TORC1 of its potential to gain access to and phosphorylate Lst4. This was indeed the case, as we could not detect any phosphorylation of Lst4-Ser^{523} in the absence of Lst7, while TORC1 was still able, albeit with reduced activity as expected, to phosphorylate Sch9-Thr^{737} in the same strain (Figure 2F).

TORC1 Phosphorylation Sites Critically Control Lst4 Localization

To analyze the role of TORC1-dependent phosphorylation of Lst4, we next studied the properties of Lst4, Lst4^{12A}, and the Lst4^{5D} variant, which carried phosphomimetic Asp (D) substitutions of those 5 Ser residues (i.e., Ser^{484}, Ser^{498}, Ser^{523}, Ser^{547}, and Ser^{550}) that our mass spectrometry analyses identified as the most probable TORC1-dependent phosphorylation sites within Lst4 (Figure 2C). In line with our previous results (Péli-Gulli et al., 2015), amino acid starvation (or rapamycin treatment) rapidly provoked a strong enrichment of Lst4-ENVY at the vacuolar membrane, which was reversed in starved cells when refed with glutamine (Figure 3A). Under the same conditions, Lst4^{12A}-ENVY was found constitutively enriched at, while Lst4^{5D} was invariably absent from the vacuolar membrane (Figure 3A). Importantly, both variants Lst4^{12A} and Lst4^{5D} associated normally with Lst7 within cells (Figure 3B). Moreover, they dictated the localization of Lst7, as Lst7-GFP was constitutively tethered to the vacuolar membrane in Lst4^{12A}-expressing cells, while it was unable to reach the vacuolar membrane

1NM-PP1 ATP analog-sensitive *sch9*^{as} allele (*lst4Δ sch9*^{as}) co-expressed (+), or not (-), Lst4-V5 and the Sch9 substrate Maf1-HA$_3$ from plasmids. Cells were grown exponentially (EXP) in SC and then subjected (+), or not (-), to rapamycin (RAP) and/or 1NM-PP1 treatments for the indicated times. Lst4-pSer^{523}, Lst4-V5, Maf1-HA$_3$, Sch9-pThr^{737}, and Sch9 were monitored by immunoblot analysis using anti-Lst4-pSer^{523}, anti-V5, anti-HA$_3$, anti-Sch9-pThr^{737}, and anti-Sch9 antibodies, respectively. P, phosphorylated isoforms of Maf1-HA$_3$. See also Figure S2.

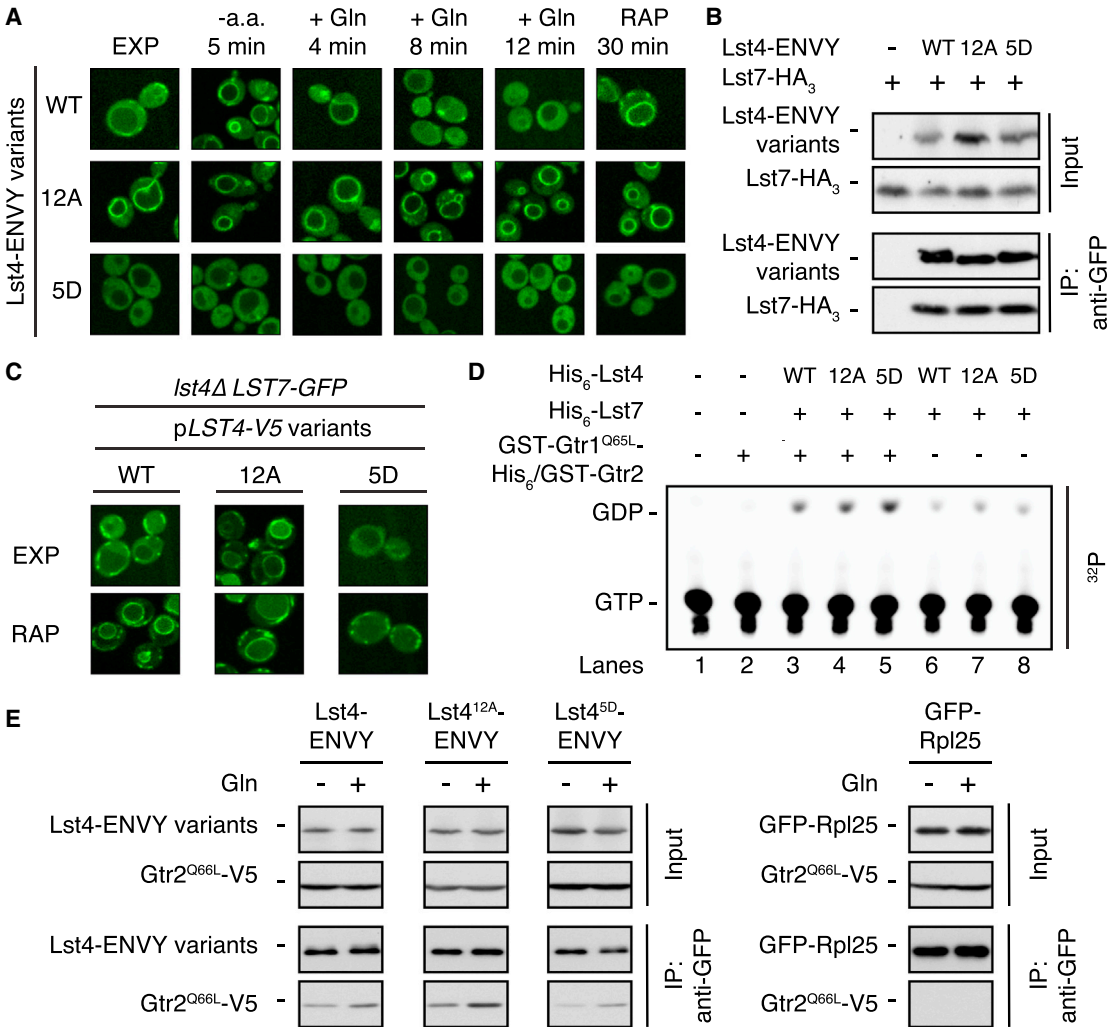

Figure 3. TORC1 Phosphorylation Sites Critically Control Lst4 Localization

(A) Lst4^{12A}-ENVY (12A) is stably enriched at, while Lst4^{5D}-ENVY (5D) is unable to reach the vacuolar surface. Cells (*lst4Δ*) expressing the indicated Lst4-ENVY variants from their genomes were grown exponentially in SC (EXP), treated with rapamycin (RAP), or starved of amino acids (-a.a.) and refed with 3 mM glutamine (+ Gln) for the indicated times.

(B) Lst4^{12A} and Lst4^{5D} normally associate with Lst7. Cells (*lst4Δ lst7Δ*) expressing, or not (-), Lst4-ENVY (WT), Lst4^{12A}-ENVY (12A), or Lst4^{5D}-ENVY (5D) from their genomes together with plasmid-encoded Lst7-HA$_3$ (+) were grown exponentially in SC. Lysates (input) and anti-GFP immunoprecipitates (IP: anti-GFP) were analyzed by immunoblotting using anti-HA and anti-GFP antibodies.

(C) Lst4 phospho-variants dictate Lst7-GFP localization. Cells (*lst4Δ LST7-GFP*) expressing plasmid-encoded Lst4-V5, Lst4^{12A} -V5, or Lst4^{5D}-V5 were grown exponentially (EXP) in SC or treated with rapamycin for 30 min (RAP).

(D) Lst4 (WT), Lst4^{12A} (12A), and Lst4^{5D} (5D) stimulate the GTPase activity of Gtr2 to a similar extent when combined with Lst7. Purified GST-Gtr1^{Q65L}-His$_6$/GST-Gtr2 (200 nM) were pre-loaded with (α-^{32}P) GTP and incubated for 20 min in the presence (WT, +; 12A, +; 5D, +; lanes 3–5) or absence (-, -; lane 2) of the different Lst4-Lst7 heterodimers (each 100 nM). The extent of (α -^{32}P) GTP hydrolysis to (α-^{32}P) GDP was measured by thin-layer chromatography (TLC), of which one representative autoradiograph is shown. In control experiments, (α-^{32}P) GTP was incubated alone (lane 1) or only together with the Lst4-Lst7 heterodimer variants (lanes 6–8). Notably, Lst4-Lst7, Lst4^{12A}-Lst7, and Lst4^{5D}-Lst7 did not significantly differ in their capacities to enhance the GTP hydrolytic activity of Gtr2, as the respective GAP-mediated fold increase of GTP hydrolysis was 31.5 ± 2.7 for Lst4-Lst7, 38.5 ± 12.0 for Lst4^{12A}-Lst7, and 41.4 ± 16.6 for Lst4^{5D}-Lst7 (n = 3; ±SD).

(E) Exponentially growing *lst4Δ gtr1Δ gtr2Δ* and *gtr1Δ gtr2Δ* cells expressing the Lst4-ENVY variants and GFP-Rpl25 (control), respectively, as well as Gtr1-HA$_3$ and Gtr2^{Q66L}-V5, were starved for amino acids (5 min; -) and then restimulated with glutamine (4 min; Gln; +). Lysates (input) and anti-GFP immunoprecipitates (IP: anti-GFP) were analyzed by immunoblotting using anti-GFP and anti-V5 antibodies. The corresponding interactions with wild-type Gtr2 were similar to, but overall weaker than, the ones with the preferred Lst4 substrate Gtr2^{Q66L} (Péli-Gulli et al., 2015; data not shown).

even in rapamycin-treated, Lst4^{5D}-expressing cells (Figure 3C). Interestingly, all heterodimeric variants normally stimulated the GTPase activity of Gtr2 when assayed in vitro (Figure 3D). Within cells, however, glutamine refeeding expectedly over-stimulated the interaction between Lst4^{12A} and GTP-locked Gtr2^{Q66L}, while Lst4^{5D} was significantly compromised in its

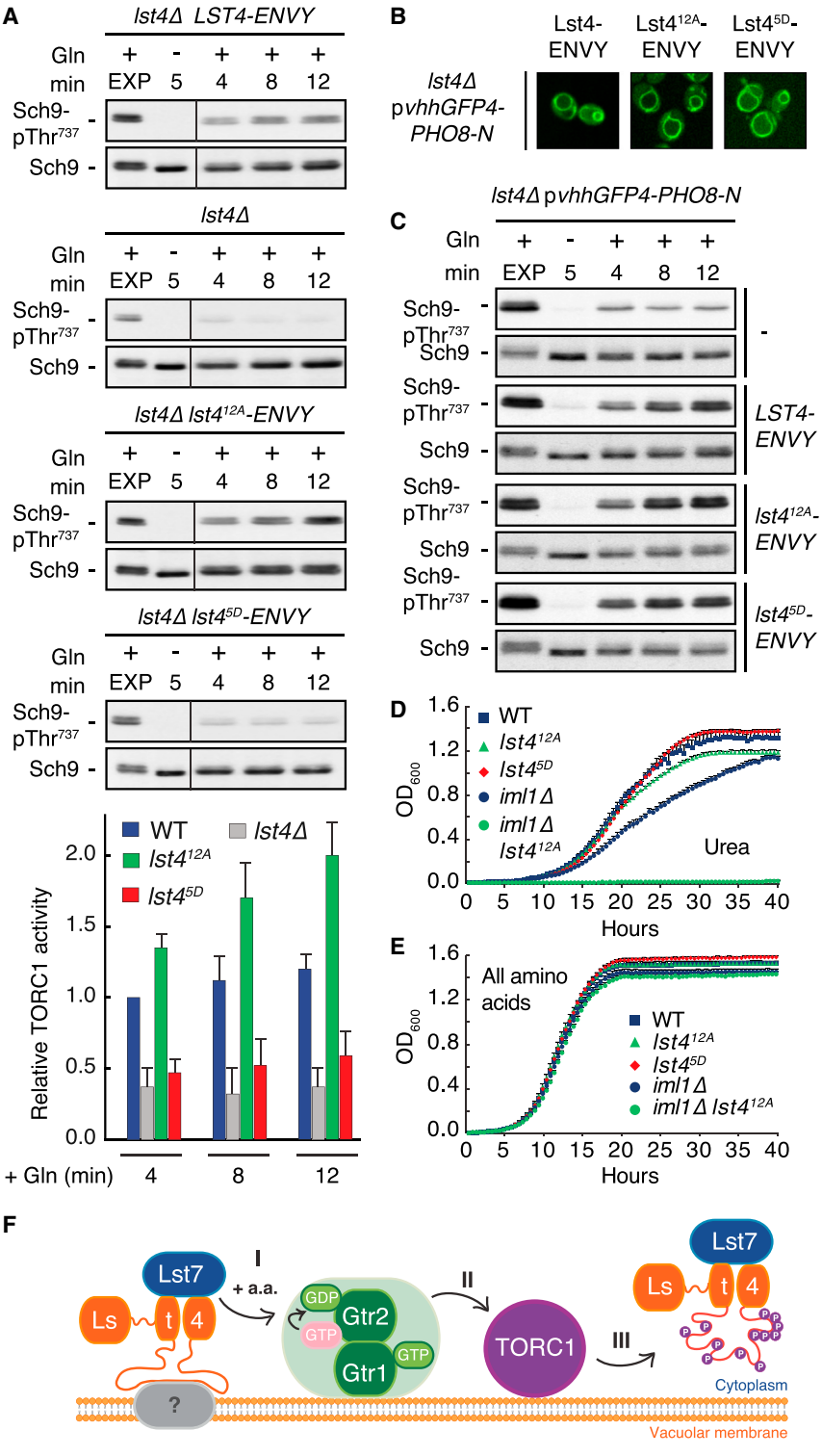

Figure 4. Homeostatic Control of TORC1 in Response to Amino Acids Relies on Feedback Inhibition of the Rag GTPase GAP Complex Lst4-Lst7

(A) Lst4, Lst4^{12A}, and Lst4^{5D} exhibit distinct TORC1 activation properties in vivo. Cells (*lst4Δ*) expressing, or not, the indicated Lst4-ENVY variants from their genomes were grown and tested for their TORC1 activities as in Figure 2A. Relative TORC1 activities were determined as the ratio of Sch9-pThr^{737}/Sch9 in *lst4Δ LST4-ENVY* (WT), *lst4Δ*, *lst4Δ lst4^{12A}-ENVY* (*lst4^{12A}*), and *lst4Δ lst4^{5D}-ENVY* (*lst4^{5D}*) cells, normalized to that of WT cells after 4 min of glutamine (Gln) refeeding, and presented in a bar graph as mean ± SD (n = 3).

(B) Artificial vacuolar membrane anchorage of Lst4-ENVY variants. Vacuolar membrane tethering of Lst4-ENVY variants in *lst4Δ* cells (grown exponentially on SC) was achieved through overexpression of the Pho8 N terminus fused to vhhGFP4, an anti-GFP single-domain antibody fragment (Caussinus et al., 2011).

(C) Constitutive vacuolar membrane tethering of Lst4^{5D}-ENVY suppresses its defect in mediating TORC1 activation by amino acid. Cells (*lst4Δ*) overexpressing vhhGFP4-Pho8-N and co-expressing, or not (-), the indicated Lst4-ENVY variants were cultured and assayed for TORC1 activation as in (A).

(D and E) Expression of the Lst4^{12A} variant impairs growth on nitrogen-poor medium. Growth curves of *lst4Δ* cells expressing Lst4-ENVY, Lst4^{12A}-ENVY, or Lst4^{5D}-ENVY, or of *iml1Δ lst4Δ* cells expressing Lst4-ENVY or Lst4^{12A}-ENVY from their genomes (relevant genotypes are indicated). Strains were either grown in SD containing 2.5 mM urea instead of ammonium sulfate (D) or in SC containing a mixture of all amino acids (E) as nitrogen source. Growth was monitored using a Bioscreen C reader set at 30°C with readings (OD_{600}) taken every 30 min. The experiments were performed independently three times with technical quadruplicates. Data are means + SD.

(F) TORC1 feedback inhibits Lst4-Lst7. For details, see text.

TORC1-Mediated Control of Lst4 Localization Is Part of a Negative Feedback Mechanism

Given that the Lst4-Lst7 complex is critical for amino acid-dependent TORC1 activation, we reasoned that the aberrant subcellular localization of Lst4^{12A} or Lst4^{5D} might affect TORC1 activity in vivo. Indeed, the Lst4^{12A} mutant allele significantly hyperstimulated TORC1 in glutamine-refed cells (Figure 4A). Conversely, cells expressing the Lst4^{5D} allele exhibited, like *lst4Δ* cells, a strong defect in TORC1 reactivation when refed with glutamine subsequent to amino acid starvation (Figure 4A). As expected on the basis of our in vitro GAP assays (Figure 3D), both Lst4 alleles (i.e., Lst4^{12A} and Lst4^{5D}) were equally competent in vivo to reactivate TORC1 upon glutamine refeeding when they were capacity to bind Gtr2^{Q66L} under the same conditions (Figure 3E). Taken together, our results are all consistent with a model in which TORC1-dependent phosphorylation of Lst4 primarily serves to dislodge the Lst4-Lst7 GAP complex from the vacuolar membrane.

artificially and constitutively tethered to the vacuolar membrane (Figures 4B and 4C). Thus, the vacuolar membrane localization of Lst4 (combined with Lst7) is a pivotal process that is required for Rag GTPase-dependent activation of TORC1 by amino acids, and TORC1 inhibits (in a feedback loop) the Lst4-Lst7 Rag GTPase GAP primarily by favoring its dispersal from the surface of the vacuole.

Homeostatic control of TORC1 activity is important for the adaptation of cells to changing environments. Accordingly, a downshift in the quality of the nitrogen source coordinately downregulates TORC1 to induce, for instance, the expression of specific amino acid permeases and catabolic enzymes, and failure to do so (e.g., when cells express hyperactive Rag GTPases) results in cell proliferation defects on nitrogen-poor media (Binda et al., 2009; Neklesa and Davis, 2009). Consistent with this notion and the observed TORC1 activities in our *lst4* mutants (Figure 4A), we found *lst4*^{12A} cells, but not wild-type or *lst4*^{5D} cells, to exhibit a moderate but statistically significant cell proliferation defect when grown on the poor nitrogen source urea, while all strains grew equally well on a preferred nitrogen source (i.e., a mixture of all amino acids; Figures 4D and 4E). Moreover, loss of the Gtr1 GAP Iml1, which causes Gtr1 to be predominantly in its TORC1-activating GTP-bound state (Panchaud et al., 2013), caused a similar growth defect when cells were grown on urea (Figure 4D). Remarkably, the combination of *iml1Δ* (sustaining Gtr1^{GTP}) and *lst4*^{12A} (sustaining Gtr2^{GDP}) caused a dramatic synthetic growth defect that rendered cells unable to grow on urea, while they grew normally on amino acid-rich medium (Figures 4D and 4E). Appropriate feedback inhibition of the Lst4-Lst7 module by TORC1 is therefore part of a physiologically relevant adaptation program.

Taken together, our work advocates a model in which amino acid limitation triggers, through a still largely elusive mechanism, TORC1 downregulation, thereby favoring dephosphorylation and recruitment of the GAP complex Lst4-Lst7 to the vacuolar membrane (Figure 4F). In addition to being tethered proximally to Gtr2, the Lst4-Lst7 GAP further requires the presence of amino acids to be able to act on Gtr2 (Figure 4F, I), which then, in association with Gtr1, stimulates TORC1 (Figure 4F, II). Subsequent feedback inhibition of Lst4-Lst7 (Figure 4F, III), as revealed in this study, is a central element that secures the dynamic adjustment of TORC1 activity in response to amino acids. Further refinement of this model will undoubtedly depend on the identification of the protein(s) that dock Lst4 to the vacuolar membrane (Figure 4F, question mark). While we deem it possible that such a protein(s) may also be implicated in local amino acid-driven activation of the Lst4-Lst7 complex toward Gtr2, we speculate that the multiple TORC1 target residues in Lst4 might additively dictate the recognition of such a protein(s) and hence provide an additional regulatory layer to fine-tune graded TORC1 feedback responses. Finally, human FNIP1/2, like Lst4, contain a split DENN domain (Pacitto et al., 2015), and FLCN reportedly concentrates at the lysosomal surface upon mTORC1 inactivation in a human retinal pigment epithelial cell line (ARPE-19) (Martina et al., 2014), indicating that mTORC1 may use a feedback mechanism in higher eukaryotes that is analogous to the one in yeast.

EXPERIMENTAL PROCEDURES

Strains, Plasmids, and Growth Conditions

Saccharomyces cerevisiae strains and plasmids used in this study are listed in Tables S1 and S2, respectively. Exclusively prototrophic yeast strains were used throughout this study. Unless stated otherwise, yeast cells were pregrown in synthetic dropout (SD; 0.17% yeast nitrogen base, 0.5% ammonium sulfate [AS], 0.2% dropout mix [USBiological], and 2% glucose) medium to maintain plasmids, spun and diluted in synthetic complete medium (SC; SD with all amino acids, but without AS), starved of amino acids and restimulated with 3 mM glutamine as previously reported (Péli-Gulli et al., 2015). Rapamycin (LC Laboratories), cycloheximide (Sigma), and 1 NM-PP1 (Cayman Chemicals) were used at 200 ng ml^{-1}, 25 μg ml^{-1}, and 200 nM, respectively, for the times indicated.

In Vivo and In Vitro TORC1 Activity Assays

In vivo TORC1 activity was monitored as previously described (Péli-Gulli et al., 2015), making use of phosphospecific anti-Sch9-pThr^{737} and anti-Sch9 antibodies (GenScript) to probe endogenous Sch9. For in vitro kinase assays, TORC1 was TAP-purified from a Tco89-TEV-TAP-expressing yeast strain grown in YPD and treated for 10 min with cycloheximide. The extraction buffer (50 mM HEPES/NaOH [pH 7.5], 5 mM CHAPS, 400 mM NaCl, 1 mM EDTA, 0.5 mM DTT, 400 μM Pefabloc, 1× Roche complete protease inhibitor-EDTA) was used to resuspend cells that were subjected to cryogenic disruption with an MM 400 Mixer Mill (Retsch). The cleared lysate was incubated with IgG-coupled Dynabeads (Dynabeads M-270 Epoxy; Invitrogen) for 2 hr at 4°C. After washes, the TORC1 complex was eluted using 5% TEV protease. Recombinant His$_6$-tagged Lst4 variants (600 ng/30 μl reaction) were co-purified with His$_6$-tagged Lst7 and used as in vitro substrates in TORC1 kinase reactions performed according to Urban et al. (2007). Briefly, reactions were performed in kinase buffer (50 mM HEPES/NaOH [pH 7.5], 5 mM CHAPS, 400 mM NaCl, 0.5 mM DTT, phosphatase inhibitors), started by adding the ATP Mix (4.2 mM $MgCl_2$, 300 μM ATP, and 3.3 μCi [γ-^{32}P]-ATP [Hartmann Analytic, SRP-501]) and stopped by adding SDS-PAGE sample buffer. Proteins were separated by SDS-PAGE, stained with Sypro Ruby (Sigma), and analyzed using a phosphorimager (Typhoon FLA 9500; GE Healthcare).

Mass Spectrometry Analyses

Mass spectrometric measurements were performed on a Q Exactive Plus mass spectrometer coupled to an EasyLC 1000 (Thermo Fisher Scientific). Prior analysis phosphopeptides were enriched by TiO_2. The mass spectrometry raw data files were analyzed using MaxQuant software (Cox and Mann, 2008), version 1.4.1.2, using a Uniprot *S. cerevisiae* database from March 2016 containing common contaminants such as keratins and enzymes used for in-gel digestion.

Miscellaneous

GAP assays were performed as previously detailed (Péli-Gulli et al., 2015). Co-immunoprecipitation and fluorescence microscopy experiments were also carried out as described before (Panchaud et al., 2013). Phosphorylated forms of tagged-Lst4 were detected by electrophoresis on a 6% SDS-PAGE gel containing 20 μM Phos-tag (Wako) followed by immunoblotting with anti-GFP antibodies (Roche) or by classical SDS-PAGE and immunoblotting using anti-Lst4-pSer^{523} antibodies generated by GenScript and anti-V5 antibodies (Thermo Fisher Scientific). A standard protocol was applied to in vitro dephosphorylate immunoprecipitated Lst4-ENVY with λ-phosphatase (New England Biolabs).

SUPPLEMENTAL INFORMATION

Supplemental Information includes two figures and three tables and can be found with this article online at http://dx.doi.org/10.1016/j.celrep.2017.06.058.

AUTHOR CONTRIBUTIONS

Conceptualization, M.-P.P.-G., S.R., and C.D.V.; Methodology, M.-P.P.-G., S.R., Z.H., J.D., and C.D.V.; Investigation, M.-P.P.-G., S.R., and Z.H.;

Writing – Original Draft, C.D.V.; Writing – Review & Editing, M.-P.P.-G., J.D., and C.D.V.; Funding Acquisition, Resources, & Supervision, J.D. and C.D.V.

ACKNOWLEDGMENTS

We thank Floriane Jacquier, Hélène Bloechlinger, and Yvan Meier for technical assistance and Robbie Loewith, Dieter Kressler, and Riko Hatakeyama for plasmids. This research was supported by the Canton of Fribourg and the Swiss National Science Foundation (J.D. and C.D.V.).

Received: April 10, 2017
Revised: June 2, 2017
Accepted: June 21, 2017
Published: July 11, 2017

REFERENCES

Albert, V., and Hall, M.N. (2015). mTOR signaling in cellular and organismal energetics. Curr. Opin. Cell Biol. *33*, 55–66.

Binda, M., Péli-Gulli, M.P., Bonfils, G., Panchaud, N., Urban, J., Sturgill, T.W., Loewith, R., and De Virgilio, C. (2009). The Vam6 GEF controls TORC1 by activating the EGO complex. Mol. Cell *35*, 563–573.

Caussinus, E., Kanca, O., and Affolter, M. (2011). Fluorescent fusion protein knockout mediated by anti-GFP nanobody. Nat. Struct. Mol. Biol. *19*, 117–121.

Cox, J., and Mann, M. (2008). MaxQuant enables high peptide identification rates, individualized p.p.b.-range mass accuracies and proteome-wide protein quantification. Nat. Biotechnol. *26*, 1367–1372.

Eltschinger, S., and Loewith, R. (2016). TOR complexes and the maintenance of cellular homeostasis. Trends Cell Biol. *26*, 148–159.

Hatakeyama, R., and De Virgilio, C. (2016). Unsolved mysteries of Rag GTPase signaling in yeast. Small GTPases *7*, 239–246.

Huber, A., Bodenmiller, B., Uotila, A., Stahl, M., Wanka, S., Gerrits, B., Aebersold, R., and Loewith, R. (2009). Characterization of the rapamycin-sensitive phosphoproteome reveals that Sch9 is a central coordinator of protein synthesis. Genes Dev. *23*, 1929–1943.

Jewell, J.L., Russell, R.C., and Guan, K.L. (2013). Amino acid signalling upstream of mTOR. Nat. Rev. Mol. Cell Biol. *14*, 133–139.

Jin, G., Lee, S.W., Zhang, X., Cai, Z., Gao, Y., Chou, P.C., Rezaeian, A.H., Han, F., Wang, C.Y., Yao, J.C., et al. (2015). Skp2-mediated RagA ubiquitination elicits a negative feedback to prevent amino-acid-dependent mTORC1 hyperactivation by recruiting GATOR1. Mol. Cell *58*, 989–1000.

Kim, E., Goraksha-Hicks, P., Li, L., Neufeld, T.P., and Guan, K.L. (2008). Regulation of TORC1 by Rag GTPases in nutrient response. Nat. Cell Biol. *10*, 935–945.

Liu, Q., Xu, C., Kirubakaran, S., Zhang, X., Hur, W., Liu, Y., Kwiatkowski, N.P., Wang, J., Westover, K.D., Gao, P., et al. (2013). Characterization of Torin2, an ATP-competitive inhibitor of mTOR, ATM, and ATR. Cancer Res. *73*, 2574–2586.

Martina, J.A., Diab, H.I., Lishu, L., Jeong-A, L., Patange, S., Raben, N., and Puertollano, R. (2014). The nutrient-responsive transcription factor TFE3 promotes autophagy, lysosomal biogenesis, and clearance of cellular debris. Sci. Signal. *7*, ra9.

Neklesa, T.K., and Davis, R.W. (2009). A genome-wide screen for regulators of TORC1 in response to amino acid starvation reveals a conserved Npr2/3 complex. PLoS Genet. *5*, e1000515.

Pacitto, A., Ascher, D.B., Wong, L.H., Blaszczyk, B.K., Nookala, R.K., Zhang, N., Dokudovskaya, S., Levine, T.P., and Blundell, T.L. (2015). Lst4, the yeast Fnip1/2 orthologue, is a DENN-family protein. Open Biol. *5*, 150174.

Panchaud, N., Péli-Gulli, M.P., and De Virgilio, C. (2013). Amino acid deprivation inhibits TORC1 through a GTPase-activating protein complex for the Rag family GTPase Gtr1. Sci. Signal. *6*, ra42.

Péli-Gulli, M.P., Sardu, A., Panchaud, N., Raucci, S., and De Virgilio, C. (2015). Amino acids stimulate TORC1 through Lst4-Lst7, a GTPase-activating protein complex for the Rag family GTPase Gtr2. Cell Rep. *13*, 1–7.

Petit, C.S., Roczniak-Ferguson, A., and Ferguson, S.M. (2013). Recruitment of folliculin to lysosomes supports the amino acid-dependent activation of Rag GTPases. J. Cell Biol. *202*, 1107–1122.

Powis, K., and De Virgilio, C. (2016). Conserved regulators of Rag GTPases orchestrate amino acid-dependent TORC1 signaling. Cell Discov. *2*, 15049.

Reinke, A., Chen, J.C., Aronova, S., and Powers, T. (2006). Caffeine targets TOR complex I and provides evidence for a regulatory link between the FRB and kinase domains of Tor1p. J. Biol. Chem. *281*, 31616–31626.

Sancak, Y., and Sabatini, D.M. (2009). Rag proteins regulate amino-acid-induced mTORC1 signalling. Biochem. Soc. Trans. *37*, 289–290.

Sancak, Y., Peterson, T.R., Shaul, Y.D., Lindquist, R.A., Thoreen, C.C., Bar-Peled, L., and Sabatini, D.M. (2008). The Rag GTPases bind raptor and mediate amino acid signaling to mTORC1. Science *320*, 1496–1501.

Saxton, R.A., and Sabatini, D.M. (2017). mTOR signaling in growth, metabolism, and disease. Cell *168*, 960–976.

Stracka, D., Jozefczuk, S., Rudroff, F., Sauer, U., and Hall, M.N. (2014). Nitrogen source activates TOR (target of rapamycin) complex 1 via glutamine and independently of Gtr/Rag proteins. J. Biol. Chem. *289*, 25010–25020.

Sturgill, T.W., Cohen, A., Diefenbacher, M., Trautwein, M., Martin, D.E., and Hall, M.N. (2008). TOR1 and TOR2 have distinct locations in live cells. Eukaryot. Cell *7*, 1819–1830.

Tsun, Z.Y., Bar-Peled, L., Chantranupong, L., Zoncu, R., Wang, T., Kim, C., Spooner, E., and Sabatini, D.M. (2013). The folliculin tumor suppressor is a GAP for the RagC/D GTPases that signal amino acid levels to mTORC1. Mol. Cell *52*, 495–505.

Urban, J., Soulard, A., Huber, A., Lippman, S., Mukhopadhyay, D., Deloche, O., Wanke, V., Anrather, D., Ammerer, G., Riezman, H., et al. (2007). Sch9 is a major target of TORC1 in *Saccharomyces cerevisiae*. Mol. Cell *26*, 663–674.